

Spoof-plasmon relevant one-way collimation and multiplexing at beaming from a slit in metallic grating

Semih Cakmakyapan,^{1,2,*} Andriy E. Serebryannikov,³ Humeyra Caglayan,⁴
and Ekmel Ozbay^{1,2,5}

¹Department of Physics, Bilkent University, Bilkent, 06800 Ankara, Turkey

²Nanotechnology Research Center, Bilkent University, Bilkent, 06800 Ankara, Turkey

³Hamburg University of Technology, E-3, D-21071 Hamburg, Germany

⁴Department of Electrical and Systems Engineering, University of Pennsylvania, Philadelphia, Pennsylvania 19104, USA

⁵Department of Electrical and Electronics Engineering, Bilkent University, Bilkent, 06800 Ankara, Turkey

*semihc@bilkent.edu.tr

Abstract: Diode and collimator/multiplexer functions are suggested to be combined in one device that is based on a thin metallic grating with a single subwavelength slit. A proper choice of the structural (a)symmetry of the grating can result in obtaining one-way collimation and multiplexing with a single on-axis or off-axis, or two off-axis narrow outgoing beams. It is possible due to freedom in utilizing different combinations of the excitation conditions of the spoof surface plasmons at the four grating parts – right and left front-side and right and left back-side ones. Such a combining provides one with an efficient tool to engineer one-way collimators and multiplexers with the desired characteristics. Strong asymmetry in transmission with respect to the incidence direction (forward vs backward case) can be obtained within a wide range of variation of the incident beam parameters, i.e., angle of incidence and frequency, while the outgoing radiation is concentrated within a narrow range of the observation angle variation. Most of the observed asymmetric transmission features can be qualitatively explained using the concept of the equivalent source placed inside the slit.

©2012 Optical Society of America

OCIS codes: (050.1220) Apertures; (050.1950) Diffraction gratings; (240.6690) Surface waves; (120.1680) Collimation; (120.7000) Transmission.

References and links

1. T. W. Ebbesen, H. J. Lezec, T. F. Ghaemi, T. A. Thio, and P. A. Wolf, "Extraordinary optical transmission through subwavelength hole arrays," *Nature* **391**(6668), 667–669 (1998).
2. H. J. Lezec, A. Degiron, E. Devaux, R. A. Linke, L. Martin-Moreno, F. J. Garcia-Vidal, and T. W. Ebbesen, "Beaming light from a subwavelength aperture," *Science* **297**(5582), 820–822 (2002).
3. T. Thio, K. M. Pellerin, R. A. Linke, H. J. Lezec, and T. W. Ebbesen, "Enhanced light transmission through a single subwavelength aperture," *Opt. Lett.* **26**(24), 1972–1974 (2001).
4. H. Caglayan, I. Bulu, and E. Ozbay, "Extraordinary grating-coupled microwave transmission through a subwavelength annular aperture," *Opt. Express* **13**(5), 1666–1671 (2005).
5. A. Degiron and T. W. Ebbesen, "Analysis of the transmission process through single apertures surrounded by periodic corrugations," *Opt. Express* **12**(16), 3694–3700 (2004).
6. E. Ozbay, "Plasmonics: Merging photonics and electronics at nanoscale dimensions," *Science* **311**(5758), 189–193 (2006).
7. H. Caglayan, I. Bulu, and E. Ozbay, "Beaming of electromagnetic waves emitted through a subwavelength annular aperture," *J. Opt. Soc. Am. B* **23**(3), 419–422 (2006).
8. Z. Li, H. Caglayan, E. Colak, and E. Ozbay, "Enhanced transmission and directivity from metallic subwavelength apertures with nonuniform and nonperiodic grooves," *Appl. Phys. Lett.* **92**(1), 011128 (2008).
9. N. F. Yu and F. Capasso, "Wavefront engineering for mid-infrared and terahertz quantum cascade lasers," *J. Opt. Soc. Am. B* **27**(11), B18–B35 (2010).
10. A. O. Cakmak, E. Colak, A. E. Serebryannikov, and E. Ozbay, "Unidirectional transmission in photonic-crystal gratings at beam-type illumination," *Opt. Express* **18**(21), 22283–22298 (2010).

11. A. E. Serebryannikov and E. Ozbay, "Unidirectional transmission in non-symmetric gratings containing metallic layers," *Opt. Express* **17**(16), 13335–13345 (2009).
12. M. Mutlu, A. E. Akosman, A. E. Serebryannikov, and E. Ozbay, "Diodelike asymmetric transmission of linearly polarized waves using magnetoelectric coupling and electromagnetic wave tunneling," *Phys. Rev. Lett.* **108**(21), 213905 (2012).
13. C. Menzel, C. Helgert, C. Rockstuhl, E.-B. Kley, A. Tünnermann, T. Pertsch, and F. Lederer, "Asymmetric transmission of linearly polarized light at optical metamaterials," *Phys. Rev. Lett.* **104**(25), 253902 (2010).
14. S. Cakmakyapan, A. E. Serebryannikov, H. Caglayan, and E. Ozbay, "One-way transmission through the subwavelength slit in nonsymmetric metallic gratings," *Opt. Lett.* **35**(15), 2597–2599 (2010).
15. S. Cakmakyapan, H. Caglayan, A. E. Serebryannikov, and E. Ozbay, "Experimental validation of strong directional selectivity in nonsymmetric metallic gratings with a subwavelength slit," *Appl. Phys. Lett.* **98**(5), 051103 (2011).
16. S. Kim, H. Kim, Y. Lim, and B. Lee, "Off-axis directional beaming of optical field diffracted by a single subwavelength metal slit with asymmetric dielectric surface gratings," *Appl. Phys. Lett.* **90**(5), 051113 (2007).
17. D. Z. Lin, T. D. Cheng, C. K. Chang, J. T. Yeh, J. M. Liu, C. S. Yeh, and C. K. Lee, "Directional light beaming control by a subwavelength asymmetric surface structure," *Opt. Express* **15**(5), 2585–2591 (2007).
18. Y. G. Liu, H. F. Shi, C. T. Wang, C. L. Du, and X. G. Luo, "Multiple directional beaming effect of metallic subwavelength slit surrounded by periodically corrugated grooves," *Opt. Express* **16**(7), 4487–4493 (2008).
19. Y. C. Jun, K. C. Y. Huang, and M. L. Brongersma, "Plasmonic beaming and active control over fluorescent emission," *Nat Commun* **2**, 283 (2011).
20. H. Caglayan, I. Bulu, and E. Ozbay, "Off-axis beaming from subwavelength apertures," *J. Appl. Phys.* **104**(7), 073108 (2008).
21. H. Caglayan, I. Bulu, and E. Ozbay, "Observation of off-axis directional beaming via subwavelength asymmetric metallic gratings," *J. Phys. D Appl. Phys.* **42**(4), 045105 (2009).
22. Y. Zhou, M. H. Lu, L. Feng, X. Ni, Y. F. Chen, Y. Y. Zhu, S. N. Zhu, and N. B. Ming, "Acoustic surface evanescent wave and its dominant contribution to extraordinary acoustic transmission and collimation of sound," *Phys. Rev. Lett.* **104**(16), 164301 (2010).
23. J. X. Fu, Y. L. Hua, Y. H. Chen, R. J. Liu, J. F. Li, and Z. Y. Li, "Systematic study on visible light collimation by nanostructured slits in the metal surface," *Chin. Phys. B* **20**(3), 037806 (2011).
24. S. B. Choi, D. J. Park, Y. K. Jeong, Y. C. Yun, M. S. Jeong, C. C. Byeon, J. H. Kang, Q. H. Park, and D. S. Kim, "Directional control of surface plasmon polariton waves propagating through an asymmetric Bragg resonator," *Appl. Phys. Lett.* **94**(6), 063115 (2009).
25. F. Lopez-Tejiera, S. G. Rodrigo, L. Martin-Moreno, F. J. Garcia-Vidal, E. Devaux, T. W. Ebbesen, J. R. Krenn, I. P. Radko, S. I. Bozhevolnyi, M. U. Gonzalez, J. C. Weeber, and A. Dereux, "Efficient unidirectional nanoslit couplers for surface plasmons," *Nat. Phys.* **3**(5), 324–328 (2007).
26. N. Bonod, E. Popov, L. F. Li, and B. Chernov, "Unidirectional excitation of surface plasmons by slanted gratings," *Opt. Express* **15**(18), 11427–11432 (2007).
27. I. P. Radko, S. I. Bozhevolnyi, G. Bruccoli, L. Martin-Moreno, F. J. Garcia-Vidal, and A. Boltasseva, "Efficient unidirectional ridge excitation of surface plasmons," *Opt. Express* **17**(9), 7228–7232 (2009).
28. A. Roszkiewicz and W. Nasalski, "Unidirectional SPP excitation at asymmetrical two-layered metal gratings," *J. Phys. B.* **43**(18), 185401 (2010).
29. A. Baron, E. Devaux, J.-C. Rodier, J.-P. Hugonin, E. Rousseau, C. Genet, T. W. Ebbesen, and P. Lalanne, "Compact antenna for efficient and unidirectional launching and decoupling of surface plasmons," *Nano Lett.* **11**(10), 4207–4212 (2011).
30. J. J. Chen, Z. Li, S. Yue, and Q. H. Gong, "Efficient unidirectional generation of surface plasmon polaritons with asymmetric single-nanoslit," *Appl. Phys. Lett.* **97**(4), 041113 (2010).

1. Introduction

Transmission through the subwavelength apertures in metallic screens has extensively been studied at microwave and optical frequencies for more than ten years [1]. Surrounding a single subwavelength hole or slit with corrugations enables enhancing an otherwise vanishing transmission due to surface plasmon excitations [2–4]. In line with the earlier studies, transmission through metallic gratings with a single slit can be regarded as a sequence of three rather independent processes: coupling in, transmission through the slit, and coupling out [5]. Then, corrugations placed at the input interface are mainly responsible for the transmission enhancement, while those at the exit interface do so for shaping the outgoing radiation. The surface plasmon inspired beaming belongs to the most interesting effects realizable in such structures [6–8]. It has been shown in many studies that the narrow outgoing beam(s) that are only a few degrees wide can be obtained. In particular, the possibility of narrowing the beam down to 2.7° at the half-power level has been demonstrated in [9].

Another interesting reciprocal phenomenon called *asymmetric transmission* has extensively been studied during the last years. In fact, it allows obtaining one-way, diode-like operation

regimes for the linearly polarized incident waves without the use of anisotropic or nonlinear constituents, at the price of the transmitted energy redistribution in favor of either higher diffraction orders [10, 11] or the other polarization [12, 13]. The realization of a diode-like transmission, i.e., that with a strong difference between the forward transmission (front-side incidence) and the backward transmission (back-side incidence), is one of the most intriguing effects realizable in metallic gratings with different corrugations at the input (incidence) and exit interfaces [14, 15]. Comparing to the other performances that enable asymmetric transmission, the use of thin metallic gratings with a slit opens a route to the compact performances, in which asymmetric transmission can be obtained in the beaming regime without polarization change.

However, in most of the studies, beaming regimes in metallic gratings with slits have been considered without connection to the possible asymmetric transmission regimes. For example, this concerns both on-axis [2] and off-axis [16–18] beaming regimes that have been studied at normal incidence. If the corrugations at the exit interface are symmetric regarding the slit, off-axis beaming appears while the outgoing beams are symmetric, too [18, 19]. If the corrugations are asymmetric, off-axis beaming can be obtained in a single-beam regime. Furthermore, the properly designed left-side and right-side corrugations at the exit interface enable the existence of surface plasmons that contribute to the same outgoing beam [16, 17, 20, 21]. Hence, radiation from the left and the right side collimate in sense of contributing to the same beam. However, this is not the main regime that is referred to as *collimation*, when metallic gratings with subwavelength slits/holes are considered. The same remains true concerning the studies relevant to semiconductor lasers [9] and some structures that support the acoustic surface waves [22], where collimation means, in fact, the same as *beaming*, i.e., just the ability to collect the input radiation to a single narrow outgoing beam. The possibility of *multiplexing*, i.e., sending the beams nearly in the same direction at several close microwave frequencies has been an auxiliary result of Ref [20]. Recently, a similar regime has been studied at optical frequencies, where it has been referred to as collimation [23]. For the sake of definiteness, multiplexing is here referred to as the operation regime, in which the contributions of the multiple incident waves/beams having different frequencies but the same angle of incidence are collected. We distinguish this regime from that one, in which the contributions of the individual waves/beams, which have the same frequency but different incidence angles, are collected. Here, we adopt the terminology, according to which the latter is referred to as collimation. The possibility of combining functions of collimator or multiplexer and diode in one device has not been studied yet.

Metallic gratings with different corrugations at the left and the right side of the exit interface enable asymmetry in the excitation of surface plasmons. This remains true also when the front and back interfaces are the same. Asymmetric excitation of surface plasmons at the left and the right side can be realized for both the slit containing [24, 25] and the slit-free [26–29] structures. In the latter case, surface plasmons can be *unidirectionally* excited at the slit-free incidence interface. A proper combination of the corrugation parameters and width and location of the incident beam spot often provides blocking the in-plane propagation in the unwanted direction(s). In the former case, they can be excited asymmetrically at the left and right sides, or only at one of the sides, while the corrugations are either different at the two sides or placed at one of the sides only. In this case, transmission through a subwavelength hole or slit is a necessary part of the utilized unidirectional mechanism. In fact, off-axis beaming with a single outgoing beam as that demonstrated in [16, 20] needs asymmetry of the surface plasmons with respect to the slit at the exit interface. In the structures with a single slit and without corrugations, asymmetry of surface plasmons at the left and right sides can be obtained due to the asymmetry of the slit alone [30].

In this paper, we demonstrate how diode-like transmission can be combined with collimation or multiplexing in one device. In the studied mechanism, transmission is weak for one of the two opposite incidence directions, in either the entire or a limited range of the observation angle variation. It will be shown that the one-way collimation and one-way multiplexing can be obtained in wide ranges of variation in angle of incidence, θ , and

frequency, f , respectively. To do this, we study transmission through metallic gratings with corrugations at both the input and exit sides and a single subwavelength slit, while putting the emphasis on the narrow-beam collimation and multiplexing. The incident beams are assumed to be rather wide and incident at an arbitrary θ . The metallic grating designs will be proposed that enable collecting radiation from the multiple wide beams that are incident at different θ and/or correspond to different values of f , while one-way transmission takes place. The desired number and direction(s) of propagation of the narrow outgoing beam(s), e.g., on-axis or off-axis, and directional selectivity, e.g., one-way or two-way transmission, and the desired half-power bandwidth are affected by the grating (a)symmetry and corrugation parameters. The strongly pronounced isolation between the input and the exit half-space, which is understood in the sense that the characteristics of the outgoing radiation are mainly determined by the spoof surface plasmons at the exit interface, is a necessary but not sufficient condition for this mechanism. As a result, variation of θ in a rather wide range is expected to slightly affect the basic features of the spatial distribution of the field in the exit half-space. However, estimation of the bandwidth invokes the extensive study of transmission, since the strength of coupling may strongly depend on θ .

The electromagnetic wave response will be studied for the three types of metallic grating structures with corrugations at the front and back sides and a single subwavelength slit. They are distinguished in the (a)symmetry type: (i) the entire structure has no symmetry with respect to both the vertical midplane and the horizontal midplane being along the interfaces, while either the front-side or the back-side interface may alone be symmetric with respect to the vertical midplane; (ii) there is asymmetry with respect to the both midplanes, while the interfaces are the same, i.e., the entire structure shows symmetry regarding the slit centerline; and (iii) there is asymmetry with respect to the horizontal midplane, although the entire structure is symmetric with respect to the vertical midplane. In fact, the first type is most general, whereas the second and the third one can be considered as its special cases. For the sake of definiteness, we further refer to the gratings with different corrugations at the left and the right side of either one of the or the both interfaces as *asymmetric* gratings. In turn, the gratings with the same corrugations at the left and right side of each of the interfaces are referred to as *symmetric* gratings. The presented simulation results have been obtained by using a finite-difference time-domain technique. The experimental validation has been done at microwave frequencies. Thus, the geometrical parameters used in simulations are adjusted to the microwave frequency range. Accordingly, a metal of which the gratings are made is treated as a perfect electric conductor. However, all the results are quite well upscalable at least up to terahertz frequencies.

2. Asymmetric grating with different interfaces

Let us start from the structures of the first type. Figure 1(a) shows a schematic of the metallic grating with a single subwavelength slit and grating periods $a \neq b$, $c = d$, $a \neq c$, and $b \neq c$, which we further refer to as Sample A. Here, we take $a = 22$ mm, $b = 14$ mm, $c = 16$ mm, and $d = 16$ mm, i.e., parameters are the same as in [20], where neither one-way transmission nor collimation has been considered. The slit width is 2 mm, thickness of the slit channel is 8 mm, and the groove depth is 4 mm. For the simulation purposes, the structure is assumed to be illuminated with a wide transverse magnetic (TM) Gaussian beam, i.e., magnetic field vector is parallel to the slit and grooves that are assumed to be infinitely long. The width of the Gaussian beam is 64 mm, and it is kept constant for all of the simulations. Transmission has been calculated at a distance of 50 cm from the slit centerline, which corresponds to the crossing of the horizontal and vertical midplanes, for the observation angle Θ varied in a wide range. θ is measured in the counter-clockwise direction from the normal to the incidence side. In turn, Θ is measured in the clockwise direction regarding the normal to the exit side. A schematic for the experimental setup is given in Fig. 1(b). Transmission measurements are carried out with an HP 8510C Network Analyzer and two standard horn antennae, whose operation range is between 10 GHz and 18 GHz. Source antenna is placed 20 cm away from

the sample with a fixed θ . Transmission is measured by placing a receiver antenna 50 cm away from the slit center with a rotating arm in order to investigate the angular dependence of the transmitted beam.

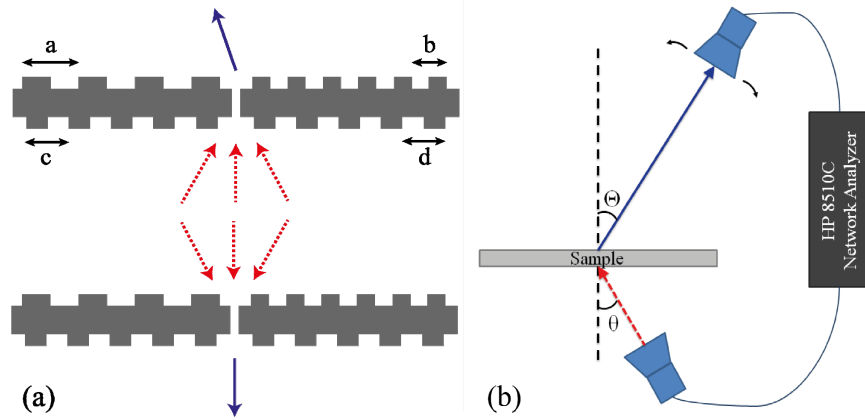


Fig. 1. (a) Geometry of Sample A and schematic of the paths of the incident (red arrows) and outgoing (blue arrows) beams that illustrates the expected collimation effect; front-side illumination (upper left plot) and back-side illumination (lower left plot), (b) Schematic of the experimental setup.

Figure 2 presents the maps of the transmitted electric field intensity T that are plotted on the (Θ, f) -plane, for $\theta = 5^\circ$ and two illumination directions (front-side and back-side illumination). The use of such a map for presentation of the transmission results allows us to directly observe the effect of simultaneous variation in f and Θ on the direction of propagation of the outgoing beam(s), and, hence, detect the existence and estimate the width of the ranges of one-way transmission. As follows from the obtained results, the resonance appears at the front-side illumination near $f = 14.5$ GHz. In this case, the transmitted beam is steered by approximately 13° due to the specific properties of the spoof plasmons excited at the asymmetric exit interface. At the back-side illumination, the resonance appears near 15.5 GHz. Now, the maximum is observed at $\Theta = 0$, that corresponds to the exit interface being symmetric with respect to the vertical midplane and, hence, to the slit. Thus, the maxima for the two opposite directions appear at the different values of Θ , i.e., the necessary condition of asymmetric transmission is fulfilled. Bandwidth of asymmetric transmission is estimated to be 2.4 GHz. From the previous studies of metallic gratings with a slit, it is known that, at the properly adjusted parameters, spoof plasmons that are excited at the input interface can be mainly responsible for the transmission enhancement through the subwavelength slit [5]. In turn, those excited at the exit interface enable the output beam shaping [5]. Thus, one can expect that the changing of θ might lead just to insignificant changes in the transmission map. This qualitatively explains why collimation of the beams that are incident at different θ and multiplexing of the incident beams that are distinguished in f to the single narrow outgoing beam can appear. The questions remain open how the coupling strength depends on θ and, hence, how wide the collimation and multiplexing ranges can be.

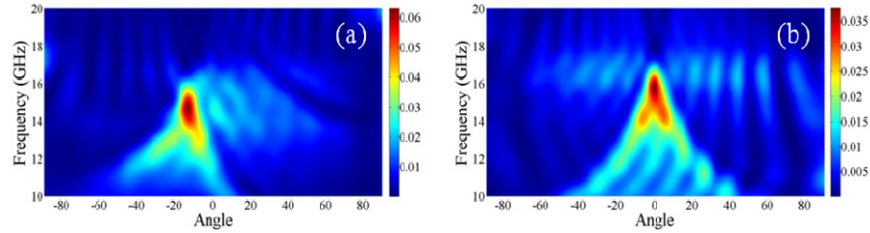


Fig. 2. Maps of electric field intensity (a.u.) for Sample A at front-side (a) and back-side (b) illumination; $\theta = 5^\circ$.

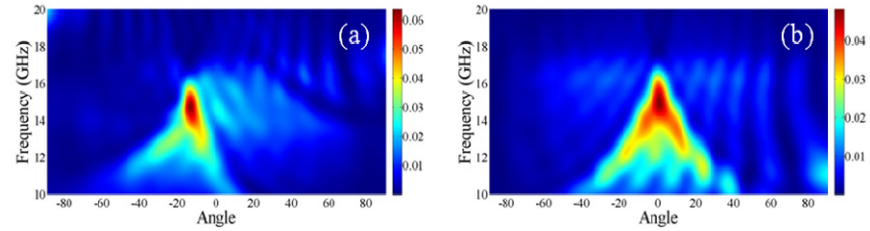


Fig. 3. Maps of electric field intensity (a.u.) for Sample A at front-side (a) and back-side (b) illumination; $\theta = -5^\circ$.

First, we check how transmission is affected by changing sign of θ . In Fig. 3, transmission maps are presented for $\theta = -5^\circ$ at the front-side and the back-side illumination. One can see that the maps for $\theta = 5^\circ$ and $\theta = -5^\circ$ are very similar. Thus, if the two wide beams of the same frequency that is taken in the vicinity of the resonance are simultaneously incident at $\theta = 5^\circ$ and $\theta = -5^\circ$, the two outgoing beams propagate in the same direction, i.e., they *collimate*. On the other hand, since directions of propagation of the outgoing beams in the vicinity of $f = 14.5$ GHz are different at the front-side and the back-side illumination, collimation can appear in a one-way manner. Furthermore, the combined one-way regime, i.e., that with radiation being collected from the incident beams which simultaneously differ in f and θ is expected to appear.

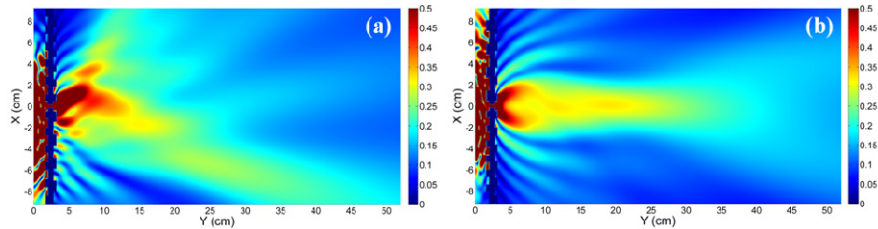


Fig. 4. Field distribution maps at $f = 14.5$ GHz for Sample A at front-side (a) and back-side (b) illumination; $\theta = 5^\circ$.

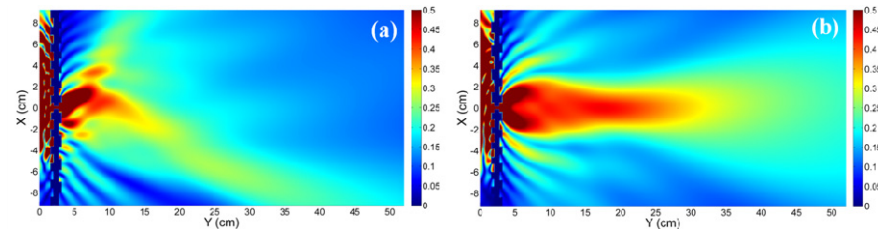


Fig. 5. Field distribution maps at $f = 14.5$ GHz for Sample A at front-side (a) and back-side (b) illumination; $\theta = -5^\circ$.

Figures 4 and 5 present the electric field distribution at the selected values of f and θ . It is seen that the change of $\text{sgn}\theta$ does not lead to new features in the field distribution. Furthermore, the outgoing (off-axis) beams in Figs. 4(a) and 5(a) seem to show nearly the same magnitude. In turn, the difference in magnitude of the outgoing beams in Figs. 4(b) and 5(b) is clearly seen. The focusing type behavior should be noticed in Figs. 4(b) and 5(b) near $Y = 20$ cm. Here, collimation and focusing can co-exist.

To explain the magnitude relevant features observed in Figs. 4 and 5, we calculated the power flow through the slit. Figure 6 presents the power flow obtained inside the slit at the horizontal midplane. In case of the front-side illumination, the results for $\theta = 5^\circ$ and $\theta = -5^\circ$ are identical. In case of the back-side illumination, they are distinguished. One can assume that the equivalent source is placed at the center of the slit, while its characteristics are determined by geometry of the input interface. Correspondingly, a symmetric input interface as in Fig. 6(a) is associated with the source that is insensitive (in terms of power flow) to the change of $\text{sgn}\theta$. In the contrast, an asymmetric input interface like that in Fig. 6(b) is associated with the source, which is affected by the change of $\text{sgn}\theta$. It is noteworthy that placing an equivalent source, say, a dipole inside a slit is well consistent with the theoretical model utilized in [19] for the nanoantenna relevant gratings. Introduction of a source inside the slit can be very useful for engineering directive radiation in the studied structures, provided that the isolation regime is realized.

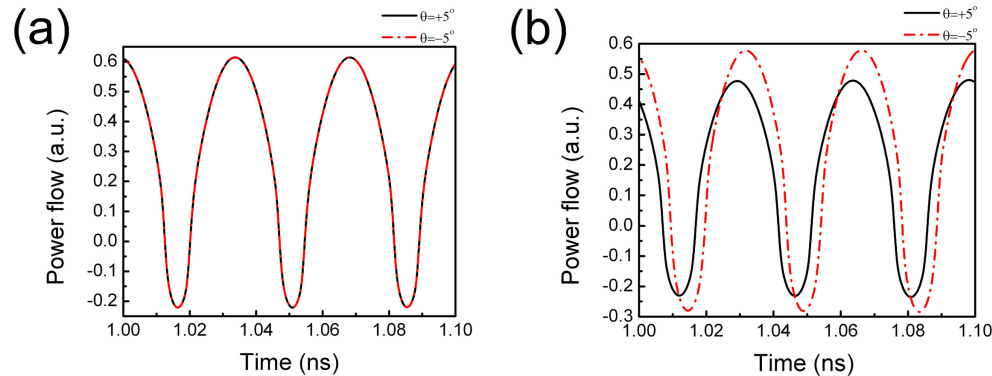


Fig. 6. Time-dependent power flow for Sample A calculated at the slit center for (a) the front-side, and (b) the back-side of the structure.

Now, let us examine the angular distribution of the electric field intensity in the exit half-space, which corresponds to a frequency near the maximum observed at the front-side illumination. In Fig. 7(a), it is presented for the four values of $\theta \geq 0$. For this illumination direction, beaming is strongly pronounced, while the θ independent maximum appears at $\Theta = -13.5^\circ$. The only difference between the curves for different θ is the beam intensity at the maximum, which decreases with increasing θ . This means, in fact, that $|\theta|$ affects the magnitude of the equivalent source if f is kept constant. At the back-side illumination, transmission is weak in the vicinity of $\Theta = -13.5^\circ$, so that the off-axis beaming with a single transmitted beam manifests itself as a *one-way* regime. In this case, the collimator and diode functions co-exist, as desired. According to the obtained transmission results, the range of θ variation, in which collimation is observed, is at least 30° wide. The obtaining of such an estimate would be impossible while being based only on the qualitative analysis in terms of symmetries and isolation. Half-power bandwidth is equal to 11° at $|\theta| = 5^\circ$ and 12° at $|\theta| = 10^\circ$, for the front-side illumination. In turn, in the vicinity of $\Theta = 0$, the contrast between the transmittances for the front-side and the back-side illumination in Fig. 7(a) is substantially smaller, thereby leading to a weakly pronounced asymmetry in transmission. Despite this, collimation still takes place in the on-axis regime at the back-side illumination, although the outgoing beam is now wider than in the off-axis regime at the front-side illumination. The

combination of the collimation and one-way beaming that appears at the front-side illumination at $-20^\circ < \Theta < -10^\circ$ is probably the most interesting regime observed for Sample A.

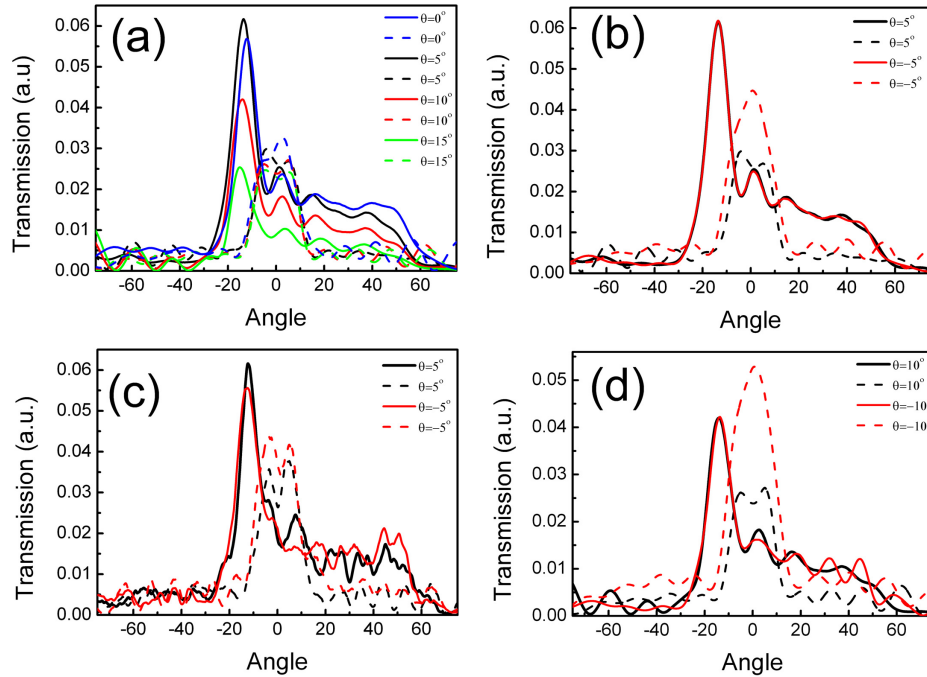


Fig. 7. Electric field intensity vs Θ at $f = 14.5$ GHz: (a) for several positive values of θ , simulation; (b) for two values of θ that differ in sign, simulation; (c) same as (b), experiment; (d) same as (b) but for larger $|\theta|$, simulation; front-side (solid lines) and back-side (dashed lines) illuminations.

Figure 7(b) presents the simulated angular distribution of the transmitted electric field intensity at the same frequency as in Fig. 7(a), but now for the two values of θ that differ in sign only. The corresponding outgoing beams collimate and, furthermore, show the same magnitudes at the maximum arising at $\Theta = -13.5^\circ$ for the front-side illumination. At the same time, the magnitudes are different when the beams collimate at $\Theta = 0$ at the back-side illumination that indicates asymmetry of the input interface. These features are in agreement with the above-used qualitative explanation based on the introduction of the equivalent source. Here, the electric field intensity at the front-side illumination is approximately six times higher than for the back-side illumination. Hence, asymmetry in transmission at changing the incidence direction to the opposite one is well pronounced. It is noteworthy that the asymmetry can be quite strong also within other Θ ranges, e.g., at $20^\circ < \Theta < 50^\circ$. However, beaming does not occur in this case. In Fig. 7(c), the experimental results for the angular distribution are presented at $f = 14.5$ GHz for $\theta = 5^\circ$ and $\theta = -5^\circ$. Good coincidence of the simulation and experimental results is observed in the vicinity of $\Theta = -13.5^\circ$, where the asymmetric transmission is best pronounced. The effect of changing sign of θ like that in Figs. 7(b) and 7(c) remains in a wide range of θ variation. For example, Fig. 7(d) presents the simulated angular distribution of the electric field intensity at $f = 14.5$ GHz for $\theta = 10^\circ$ and $\theta = -10^\circ$. The only significant difference as compared to Fig. 7(b) is that now the magnitude achieved in the beaming regime for the back-side illumination can be larger than that in the beaming regime at the front-side illumination. Note that the wide outgoing beam at $\Theta = 0$ in Fig. 7 corresponds to the region of the beam widening that is observed in Figs. 4 and 5 at $Y > 30$ cm. According to Figs. 4 and 5, the focusing effect occurs in the vicinity of $Y = 20$ cm,

where the outgoing beam at the back-side illumination is substantially narrower than in Fig. 7. However, at this distance transmission at the front-side illumination is not yet well suppressed, and, thus, asymmetry in transmission is not yet well pronounced.

A single narrow outgoing beam has been obtained in the one-way transmission regime also when several wide beams corresponding to different frequencies are incident at the same θ . This is possible because the surface plasmon resonance is rather wide, as seen in Figs. 2 and 3. An example of the angular distribution of the transmitted electric field intensity is presented in Figs. 8(a) and 8(b) for $\theta = 5^\circ$ and $\theta = 10^\circ$, respectively. At the front-side illumination, there is a slight change in the intensity maximum and its angular location is observed, at least if f is varied from 14 to 15 GHz. Hence, one-way, diode-like *multiplexing* can be obtained. A single outgoing beam can be obtained also at the back-side illumination. However, in this case, neither the well pronounced beam narrowing nor a one-way multiplexing has occurred. In the contrast to our results, those obtained for the same structure at the front-side illumination in Fig. 2 of Ref [20], are insufficient to detect one-way features and, hence, to show that the diode and multiplexer functions can be combined in one device, which is thin due to utilizing the surface plasmon resonance. The observed features allow us expecting that the one-way regime can be obtained also for the nonmonochromatic electromagnetic waves (wide beams) that have a wide frequency spectrum and are incident at rather arbitrary θ .

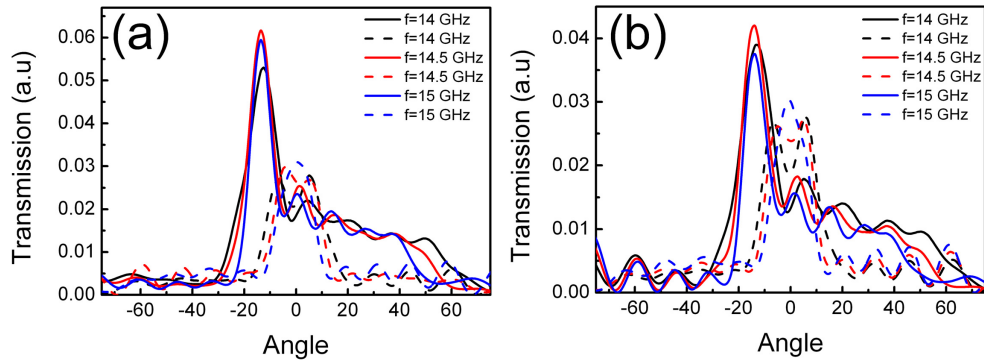


Fig. 8. Electric field intensity vs Θ at (a) $\theta = 5^\circ$ and (b) $\theta = 10^\circ$ for three frequency values, at front-side (solid lines) and back-side (dashed lines) illuminations.

3. Asymmetric grating with the same front-side and back-side interfaces

Now, let us consider the metallic grating with a slit that shows another asymmetry than Sample A. Now, $b = c$, $a = d$, $a \neq b$, and $c \neq d$. This grating represents the second type of the structures studied in this paper, see Fig. 9. Further, we refer to it as Sample B. Similarly to Sample A, it has no symmetry with respect to the vertical and horizontal midplanes. However, in contrast to Sample A, it is symmetric with respect to the slit centerline, i.e., the crossing line of the vertical and horizontal midplanes, which is perpendicular to the figure plane. We take here $a = d = 22$ mm and $b = c = 14$ mm, so that the two among the four values – a and b – are the same as for Sample A. We restrict our consideration to the case of $\theta = 0$. The results are always the same, regardless of whether the structure is illuminated from the front or the back side. The map of the transmitted electric field intensity is presented in Fig. 10(a). The resonance is observed in the vicinity $f = 14.5$ GHz. It is nearly the same as for Sample A at the front-side illumination, because Sample A and Sample B have the same exit interface. The observed behavior is well consistent with the expected dominant role played by the exit interface in shaping of the outgoing radiation. The maximum occurs now at $\Theta = -12^\circ$. The angular distribution is shown in Fig. 10(b) for the selected frequency values. The angle,

at which the intensity is maximal, is nearly the same while f varied from 14 to 15 GHz. Hence, the off-axis multiplexing is obtained here.

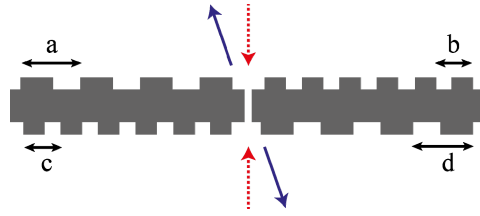


Fig. 9. Geometry of Sample B and schematic of the paths of the input (red arrows) and outgoing (blue arrows) beams.

However, as seen in Figs. 9 and 10, the beaming is not one-way. Minimization of the intensity beyond the Θ range that corresponds to the beaming (vicinity of $\Theta = -12^\circ$), e.g., at $-5^\circ < \Theta < 60^\circ$, would be important for obtaining the reversible operation regime. In this regime, two beams that are normally incident on the front and back sides should create the outgoing radiation in the directions, which are distinguished from those where the opposite-side incident beams come from. This can be done by proper optimization of the grating geometry. As a result, one might expect obtaining two-way collimation without affecting a source associated with the opposite-side radiation. The said above remains true for multiplexing. A similar problem, i.e., suppression of parasitic radiation beyond the Θ range, in which the beaming appears, exists and, therefore, should be solved also for the other type of asymmetric gratings that keep symmetry with respect to the horizontal midplane, i.e., $a = c$, $b = d$, $a \neq b$, and $c \neq d$. Also these gratings should enable protection of the opposite-side source. A comparison of the results of Sec. 2 and Sec. 3 clearly illustrates the roles played by the (a)symmetry of the exit interface and that of the entire structure in combining asymmetric transmission and off-axis beaming.

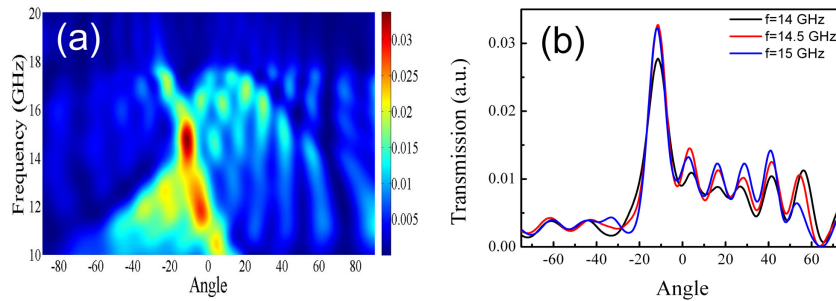


Fig. 10. Map of the transmitted electric field intensity on the (Θ, f) -plane (a) and its distribution over Θ at $\theta = 0$ (b), for Sample B.

4. Symmetric grating with different front-side and back-side interfaces

The third type of the structures studied here is represented by a metallic grating with a subwavelength slit that has corrugations being symmetric with respect to the vertical midplane but asymmetric with respect to the horizontal midplane, see Fig. 11. This structure is referred to as Sample C. In order to provide connection to our earlier studies that have not been related to collimation and multiplexing, we take here $a = b = 26$ mm and $c = d = 16$ mm, i.e., the same parameters as in [14, 15]. On the other hand, it differs from Sample A only in the grating periods at the back-side interface. Due to the specific choice of a , b , c , and d , $T(\Theta) = T(-\Theta)$ at $\theta = 0$, regardless of the illumination side. However, transmission may strongly depend on the change of the illumination side at $\theta = \text{const}$.

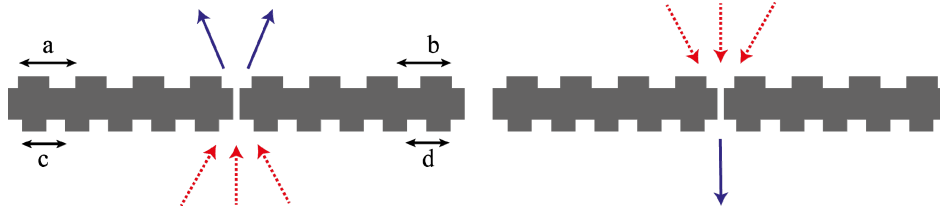


Fig. 11. Geometry of Sample C and schematic of the paths of the input (red arrows) and outgoing (blue arrows) beams; front-side illumination (left plot) and back-side illumination (right plot).

The obtained simulation results show that the diode-like, one-way collimation may appear in a wide range of θ variation. As an example, Figs. 12 and 13 present the maps of the transmitted electric field intensity for $\theta = 10^\circ$ and $\theta = -10^\circ$, respectively. Similarly to Figs. 2 and 3, change of $\text{sgn}\theta$ just slightly affects the map for both the front-side and the back-side illumination. For the former, the resonance is observed at $f = 9.5$ GHz and $\Theta = 0$. Bandwidth for this frequency regime is estimated to be 1.5 GHz, and for the other band at 14.5 GHz, the bandwidth is 1.2 GHz. At higher frequencies, the off-axis beaming occurs that is characterized by the two symmetrically outgoing narrow beams, so that the splitting function is combined here with the diode and collimator functions. For the latter, the well pronounced beaming takes place only in the vicinity of $\Theta = 0$, for the resonance arising at $f = 16$ GHz. The smaller the frequency, the wider is the range of Θ variation, in which the transmitted wave energy is localized. Similar maps have been obtained (not shown) for the values of $|\theta|$ that are distinguished from that in Figs. 12 and 13. The efficient one-way collimation occurs at least if θ is varied from -30° to 30° . It is noteworthy that the results of Refs [14, 15] are not sufficient for concluding that the one-way transmission regime may co-exist with collimation in a wide θ range.

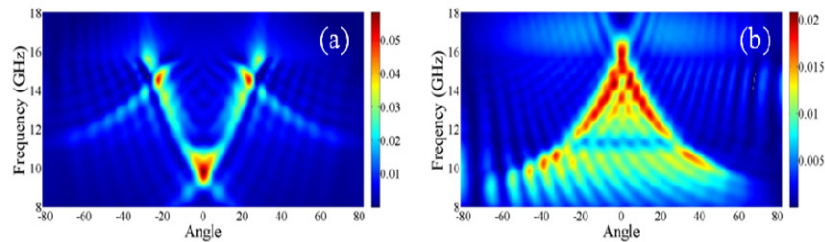


Fig. 12. Maps of the transmitted electric field intensity for Sample C at front-side (a) and the back-side (b) illumination; $\theta = 10^\circ$.

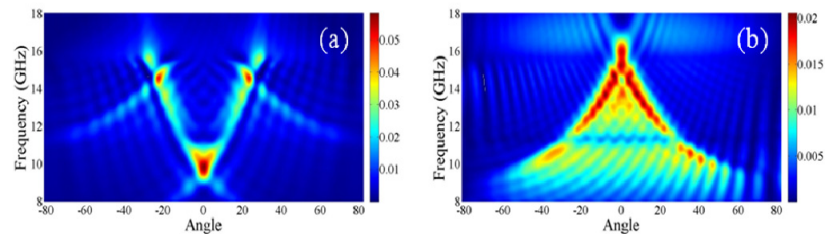


Fig. 13. Same as Fig. 12 but for $\theta = -10^\circ$.

Figure 14 presents the Θ -dependence of the transmitted electric field intensity at the two selected frequencies, which correspond to the high- T spots in Figs. 12(a) and 13(a). A more than fivefold forward-to-backward transmission contrast is observed in Fig. 14(a) in the single-beam on-axis regime. A more than tenfold contrast is observed in Fig. 14(b) in the

two-beam off-axis regime. It is seen that the change of sign of θ does not lead to a valuable change of the intensity in the two-beam off-axis regime, i.e., at $\Theta = 0$ in Fig. 14(a) and near $|\Theta| = 20^\circ$ in Fig. 14(b). Thus, the dual-band, one-way collimation can be obtained for Sample C, since the on-axis and off-axis one-way beaming scenarios may be realized in the same structure at the two different frequency ranges. Furthermore, the triple-band one-way collimation can be obtained by using the third band in the vicinity of $f = 16$ GHz, where the maximum is observed at $\Theta = 0$ for the back-side illumination, see Figs. 12(b) and 13(b). The main difference as compared to Fig. 7 is that now the single-beam one-way collimation appears only for the on-axis beaming scenario, while the off-axis scenario results in splitting into the two symmetrically outgoing beams. Similarly to Sample A and Sample B, multiplexing can be obtained at $\theta = \text{const}$. The explanation in terms of the equivalent source as that used in Sec. 2 is expected to be valid for Sample C, too.

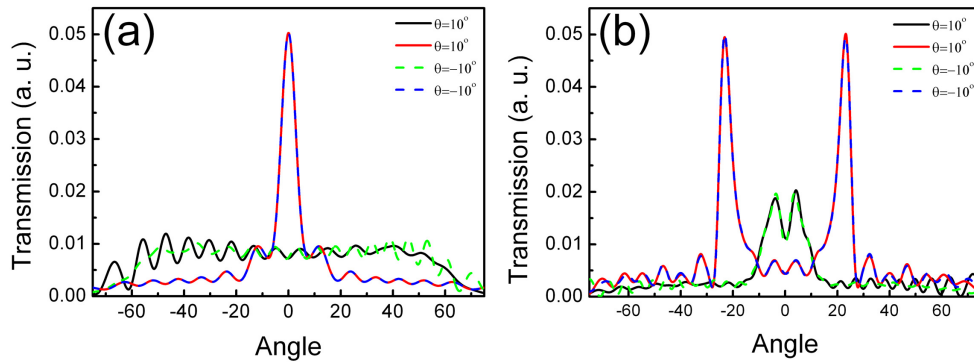


Fig. 14. Transmitted electric field intensity vs Θ for Sample C at (a) $f = 9.5$ GHz and (b) $f = 14.5$ GHz; red solid and blue dashed lines represent front-side illumination; black solid and green dashed lines represent back-side illumination.

Finally, Table 1 summarizes the basic features of the grating symmetry and the relevant transmission features for the studied performances. Connection between the symmetry properties and the ability of one-way collimation is clearly seen.

Table 1. Symmetries and one-way collimation regimes for Samples A, B, and C. Signs + and – indicate that the corresponding symmetry or collimation regime exists or does not exist, respectively, for each of the three samples.

	A	B	C
Symmetry			
Entire structure, with respect to the vertical midplane	–	–	+
Entire structure, with respect to the horizontal midplane	–	–	–
Entire structure, with respect to the crossing line of the vertical and horizontal midplanes	–	+	–
Front-side interface, with respect to the vertical midplane	+	–	+
Back-side interface, with respect to the vertical midplane	–	–	+
One-way collimation regime			
Single off-axis beam	+	–	–
Two symmetric off-axis beams (splitting)	–	–	+
Single on-axis beam	–	–	+

5. Conclusions

In this paper, we demonstrated that for multiple wide incident beams, which are distinguished in the angle of incidence or frequency, the beaming, collimation, and multiplexing, on the one hand, and one-way, diode-like transmission, on the other hand, can be combined in one device. The suggested compact performances based on metallic gratings that support spoof surface plasmons can replace, in fact, a sequence of two or more devices. Isolation that is

understood in the sense that the spatial distributions of the field in the input and the exit half-space are quite independent of each other is a key requirement for obtaining of one-way collimation and multiplexing. One more requirement is that the resonances are not sharp. It is fulfilled for the typical spoof surface plasmons. This is important since the contributions of the individual incident beams must be collectable, even if the frequencies of the incident beams are distinguished. The obtained results demonstrate how (a)symmetry type and relevant difference in the conditions of spoof plasmon excitation at the four grating sides (right front-side, left front-side, right back-side, and left back-side) affect the number and directions of the outgoing beam(s). In particular, for the structures with an asymmetric exit interface, a one-way transmission has been obtained due to the single, off-axis, forward transmitted beam, i.e., the backward transmission is rather weak within a limited range of the observation angle variation. Transmission maps plotted on the frequency-observation-angle plane for the incidence angles, which differ in sign only, are very similar, provided that the input interface is symmetric with respect to the slit. In this case, contributions of the corresponding incident wide beams into the narrow outgoing beam can show the same magnitude at and around the transmission maximum. For the structures with the exit interface being asymmetric with respect to the slit, one-way multiplexing can also occur in the single-beam off-axis regime. For the structures with a symmetric exit interface, the two resulting off-axis beams, or a single on-axis beam appear in a one-way regime a wide range of the observation angle variation. As a result, one-way, dual-band collimation can be obtained. The proposed structures can be utilized to collect contributions from different waves/sources, e.g., in sensing applications.

Acknowledgments

This work is supported by the projects DPT-HAMIT, ESF-EPIGRAT, EU-N4E, NATO-SET-181, TUBITAK under Project Nos., 107A004, 107A012, 109E301. A.E.S. thanks the Deutsche Forschungsgemeinschaft for support of this work under Project Nos., SE1409/2-1 and SE1409/2-2. One of the authors (E.O.) also acknowledges partial support from the Turkish Academy of Sciences.